RESEARCH ARTICLE

Human Mutation

OFFICIAL JOURNAL
HGVS
HUMAN GENOME VARIATION SOCIETY
www.hgvs.org

Clinical and Radiographic Features of the Autosomal Recessive form of Brachyolmia Caused by *PAPSS2* Mutations

Aritoshi Iida,[1†] Pelin Özlem Simsek-Kiper,[2†] Shuji Mizumoto,[3†] Touma Hoshino,[3] Nursel Elcioglu,[4] Eva Horemuzova,[5] Stefan Geiberger,[6] Gozde Yesil,[7] Hülya Kayserili,[8] Gülen Eda Utine,[2] Koray Boduroglu,[2] Shigehiko Watanabe,[9] Hirofumi Ohashi,[9] Yasemin Alanay,[10] Kazuyuki Sugahara,[3] Gen Nishimura,[11] and Shiro Ikegawa[1*]

[1]*Laboratory for Bone and Joint Diseases, Center for Integrative Medical Science, RIKEN, Tokyo, Japan;* [2]*Clinical Genetics Unit, Ihsan Dogramaci Children's Hospital, Hacettepe University, Ankara, Turkey;* [3]*Laboratory of Proteoglycan Signaling and Therapeutics, Graduate School of Life Science, Hokkaido University, Sapporo, Japan;* [4]*Department of Pediatric Genetics, Marmara University Pendik Hospital, Istanbul, Turkey;* [5]*Department of Women's and Children's Health, Karolinska Institutet, & Paediatric Endocrinology Unit, Karolinska University Hospital, Stockholm, Sweden;* [6]*Department of Paediatric Radiology, Karolinska University Hospital Solna, Stockholm, Sweden;* [7]*Bezmialem Vakif University, Faculty of Medicine, Department of Medical Genetics, Fatih, Istanbul, Turkey;* [8]*Medical Genetics Department, Istanbul Medical Faculty, Istanbul University, Istanbul, Turkey;* [9]*Division of Medical Genetics, Saitama Children's Medical Center, Saitama, Japan;* [10]*Department of Pediatrics, Acibadem University School of Medicine, Istanbul, Turkey;* [11]*Department of Pediatric Imaging, Tokyo Metropolitan Children's Medical Center, Fuchu, Japan*

Communicated by Ming Qi

Received 6 April 2013; accepted revised manuscript 25 June 2013.
Published online 3 July 2013 in Wiley Online Library (www.wiley.com/humanmutation). DOI: 10.1002/humu.22377

ABSTRACT: Brachyolmia is a heterogeneous skeletal dysplasia characterized by generalized platyspondyly without significant long-bone abnormalities. Based on the mode of inheritance and radiographic features, at least three types of brachyolmia have been postulated. We recently identified an autosomal recessive form of brachyolmia that is caused by loss-of-function mutations of *PAPSS2*, the gene encoding PAPS (3′-phosphoadenosine 5′-phosphosulfate) synthase 2. To understand brachyolmia caused by *PAPSS2* mutations (*PAPSS2*-brachyolmia), we extended our *PAPSS2* mutation analysis to 13 patients from 10 families and identified homozygous or compound heterozygous mutations in all. Nine different mutations were found: three splice donor-site mutations, three missense mutations, and three insertion or deletion mutations within coding regions. In vitro enzyme assays showed that the missense mutations were also loss-of-function mutations. Phenotypic characteristics of *PAPSS2*-brachyolmia include short-trunk short stature, normal intelligence and facies, spinal deformity, and broad proximal interphalangeal joints. Radiographic features include platyspondyly with rectangular vertebral bodies and irregular end plates, broad ilia, metaphyseal changes of the proximal femur, including short femoral neck and striation, and dysplasia of the short tubular bones. *PAPSS2*-brachyolmia includes phenotypes of the conventional clinical concept of brachyolmia, the Hobaek and Toledo types, and is associated with abnormal androgen metabolism.
Hum Mutat 34:1381–1386, 2013. © 2013 Wiley Periodicals, Inc.

KEY WORDS: brachyolmia; *PAPSS2*; phenotype; androgen excess

Introduction

Brachyolmia is a heterogeneous group of skeletal dysplasias that primarily affects the spine [Warman et al., 2011]. Clinical and genetic heterogeneity have been reported in brachyolmia. At least three clinically well-defined types of brachyolmia are known: type 1, including the Hobaek (MIM #271530) and Toledo (MIM #271630) forms; type 2, referred to as the Maroteaux type (MIM #613678); and type 3 (MIM #113500), autosomal dominant forms. The molecular etiology of brachyolmia is variable. *TRPV4* mutations have been identified in an autosomal dominant form [Dai et al., 2010; Rock et al., 2008], whereas disease genes for autosomal recessive forms were unknown until the recent identification of *PAPSS2* mutations [Miyake et al., 2012].

PAPSS2 (MIM #603005) encodes human PAPS (3′-phosphoadenosine 5′-phosphosulfate) synthase 2, which generates PAPS by its respective sulfotransferases. PAPS is the universal sulfate donor required for sulfation of a variety of biomolecules, including glycosaminoglycans, proteins, steroid hormones (e.g., DHEA [dehydroepiandrosterone]), and various exogenous chemical compounds (e.g., pharmaceutical agents) [Lindsay et al., 2008; Mizumoto et al., 2013; Venkatachalam, 2003]. PAPSS2 plays a role in skeletal development. *Papss2* appears mainly in proliferating and differentiating chondrocytes and is strongly downregulated in hypertrophic

Additional Supporting Information may be found in the online version of this article.

†These authors contributed equally to this work.

*Correspondence to: Shiro Ikegawa, Laboratory for Bone and Joint Diseases, Center for Integrative Medical Science, RIKEN, 4-6-1 Shirokanedai, Minato-ku, Tokyo 108-8639, Japan. E-mail: sikegawa@ims.u-tokyo.ac.jp

Contract grant sponsors: Ministry of Health, Labor and Welfare (23300101 to S.I. and N.M., 23300201 to S.I.); Matching Program for Innovations in Future Drug Discovery and Medical Care, The Ministry of Education, Culture, Sports, Science and Technology, Japan (MEXT) (to K.S.); Grant-in-aid for Young Scientists (B) (23790066), The Japan Society for the Promotion of Science, Japan (to S.M.); The Japan Heart Foundation (to S.M.); Akiyama Life Science Foundation (to S.M.).

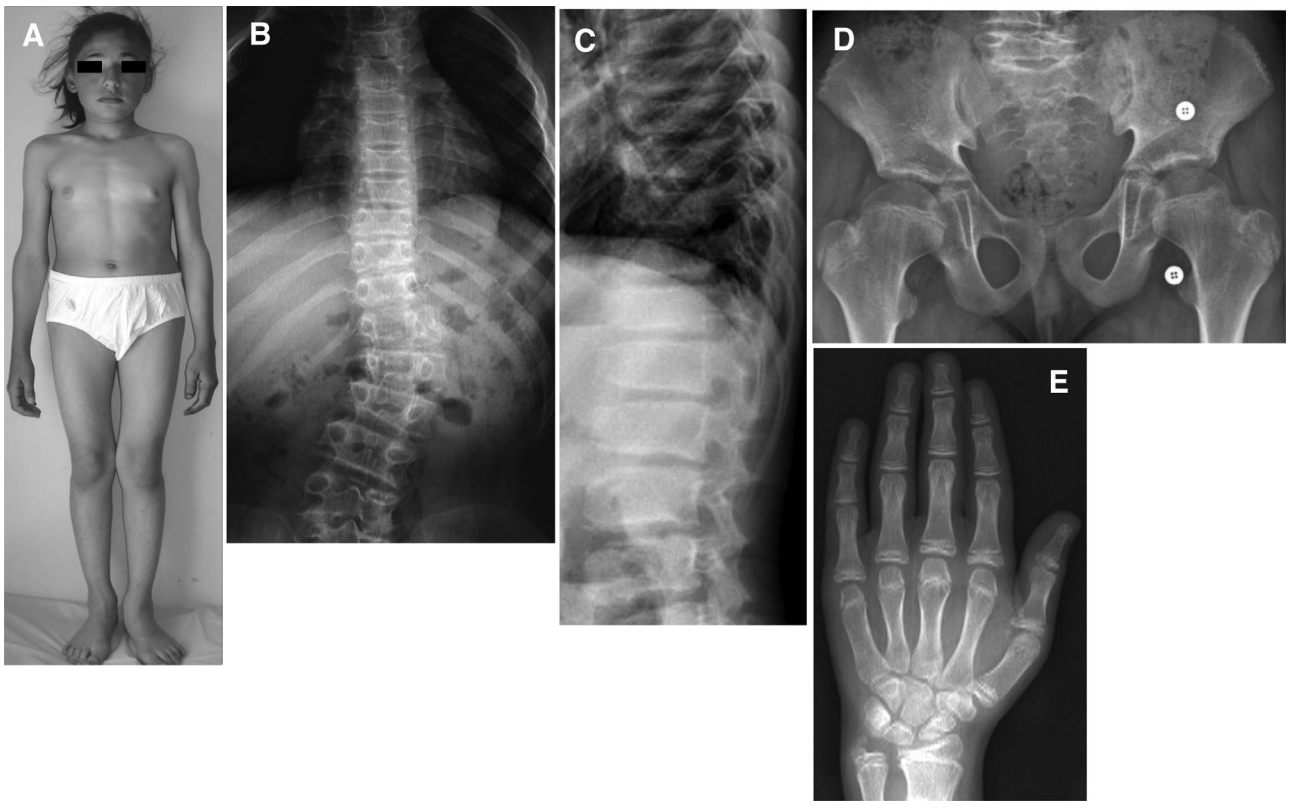

Figure 1. Clinical and radiographic features of brachyolmia caused by *PAPSS2* mutations. **A:** clinical appearance of P1 (patient 1) at the age of 14 years. Short-trunk short stature with normal facies. The upper extremities are relatively long. **B–E:** Radiographs. **B:** Spine A–P (antero–posterior). P5 at the age of 12 years. Mild lumbar scoliosis and overfaced vertebra. **C:** lateral spine. P2 at the age of 14 years. Mild flattening of vertebral bodies (rectangular vertebra) and irregular end plates. **D:** Hip A–P. P13 at the age of 9 years. Short femoral neck with longitudinal striation. **E:** Hand D–V (dorso–ventral). P5 at the age of 12 years. Short metacarpals.

chondrocytes in 13.5–16.5 dpc mouse embryos [Stelzer et al., 2007]. We have recently identified *PAPSS2* mutations by exome sequencing in a consanguineous Turkish family with brachyolmia, and confirmed *PAPSS2* mutations in three additional brachyolmia patients with different ethnic backgrounds (Japanese and Korean) but similar clinical and radiographic features [Miyake et al., 2012]. They had late-onset short-trunk short stature, normal intelligence and facies, and small hands; their radiographic features include rectangular vertebral bodies with irregular endplates, short femoral neck, and mildly shortened metacarpals. *PAPSS2* mutations were identified in both alleles in all patients, and all were nonsense mutations.

PAPSS2 mutations have also been reported to be responsible for two other overlapping, but distinct, phenotypes, that is, spondyloepimetaphyseal dysplasia (SEMD), Pakistani type [Ahmad et al., 1998], and spondylodysplasia and premature pubarche [Noordam et al., 2009]. The former is a relatively severe skeletal dysplasia that is characterized by epi-metaphyseal abnormalities in addition to spinal changes, including enlarged joints with deformity, delayed epiphyseal ossification at the hip and knees, and precocious osteoarthritic changes of the large and small joints [Ahmad et al., 1998; Faiyaz ul Haque et al., 1998]. The latter is characterized by mild platyspondyly, premature pubarche, and signs of androgen excess [Noordam et al., 2009]. Both result from loss-of-function mutations of *PAPSS2* in both alleles. Thus, *PAPSS2* is considered a causative gene of a group of skeletal dysplasias, characterized by spinal dysplasia, with a considerable variation of phenotypes. Further characterization of these phenotypes is necessary to clearly understand the clinical significance of *PAPSS2* mutations.

To understand the molecular etiology of brachyolmia caused by *PAPSS2* (*PAPSS2*-brachyolmia) and its phenotypic spectrum more precisely, we extended our analysis of *PAPSS2* mutations by examining 13 patients from 10 unrelated families. We identified homozygous or compound heterozygous *PAPSS2* mutations in all patients examined and evaluated the clinical, radiographic, and molecular features of *PAPSS2*-brachyolmia.

Materials and Methods

Subjects

Patients with the clinical and radiographic features of brachyolmia with *PAPSS2* mutations previously described [Miyake et al., 2012] were included in this study. Briefly, clinical features are short-trunk short stature that became conspicuous during childhood, normal intelligence, and normal facies (Fig. 1A). Radiographic features are rectangular vertebral bodies with irregular endplates, short femoral neck, and mildly shortened metacarpals (Fig. 1B–D). Patients with an obvious family history of dominant inheritance and/or marked epiphyseal and/or metaphyseal dysplasia were excluded.

Mutation Search

Genomic DNA was extracted from blood by standard protocol after informed consent. The exon sequences of *PAPPS2* (NM_001015880.1), with their flanking intron sequences, were

amplified by PCR from genomic DNA. PCR primer sequences and PCR conditions were as described previously [Noordam et al., 2009]. PCR products were directly sequenced for both strands using the ABI Prism 3730 × l DNA analyzer (Life Technology, Foster City, CA). The study was approved by the ethical committee of RIKEN and participating institutions.

Evaluation of Mutations

To examine the possibility of polymorphisms, the sequence changes were genotyped using the invader assay [Ohnishi et al., 2001] in more than 190 ethnicity-matched controls. The sequence changes were evaluated by public databases including dbSNP (http://www.ncbi.nlm.nih.gov/projects/SNP/), Human Gene Mutation Database (http://www.biobase-international.com/product/hgmd), PolyPhen 2 (http://genetics.bwh.harvard.edu/pph2/), and 1000 Genomes (http://www.1000genomes.org/). All mutations identified in this study are available via Leiden Open Variation Database (http://www.lovd.nl/PAPSS2).

cDNA Cloning and In Vitro Mutagenesis

The full-length *PAPSS2* cDNA was amplified using PCR, employing human lung cDNA (Clontech, Mountain View, CA) as a template, and cloned into the p3xFLAG-CMV8 vector (Sigma–Aldrich, St. Louis, MO). The missense variants were introduced into *PAPSS2* cDNA by PCR-based mutagenesis using a site-directed mutagenesis method [Heckman and Pease, 2007]. The introduced mutations were confirmed by DNA sequencing.

PAPS Synthase Enzyme Assay of PAPSS2

The expression plasmids (6 μg) were transiently transfected into COS-7 cells (Japanese Collection of Research Bioresources Cell Bank, Osaka, Japan) in a culture dish (100 mm in diameter) using FuGENE^{TM} HD transfection reagent (Promega, Madison, WI). Three days later, the culture medium (~2 mL) from the cells transfected with p3xFLAG-CMV8/PAPSS2 (wild type and mutants) was incubated with anti-FLAG affinity agarose resin (Wako, Osaka, Japan) at 4°C overnight. The enzyme-bound affinity resin was washed with 25 mM Tris–HCl, pH 7.4, containing 150 mM NaCl and 0.05% Tween-20, and was subjected to sodium dodecyl sulfate-polyacrylamide gel electrophoresis. Western blotting was carried out using the horseradish peroxidase-conjugated anti-FLAG monoclonal antibody and the ImmunoStar LD detection kit (Wako). Chemiluminescence signal was detected by LAS-4000 mini (FujiFilm, Tokyo, Japan). PAPS synthase activity was assayed by the method described previously [Fuda et al., 2002; Sugahara and Schwartz, 1979, 1982a, 1982b] with a slight modification. Briefly, the enzyme-bound ant-FLAG resin (15 μL), as an enzyme source, with 5 mM ATP and 1 mM Na_2SO_4, as substrates, were mixed in a final volume of 100 μL of 50 mM Tris–HCl, pH 8.0, 10 mM $MgCl_2$, 50 μM DTT, and 5 mM NaF. The mixtures were incubated for 2 hr at 37°C. The reaction was terminated by the addition of 1 mL of 16 mM NaH_2PO_4. Separation and quantification of the reaction products were carried out by anion exchange HPLC on an amine-bound silica PA-G column (4.6 × 150 mm^2; YMC Co., Kyoto, Japan) connected with a guard column. Authentic ribonucleotides were eluted with 16 mM NaH_2PO_4 for 10 min, followed by a linear gradient of NaH_2PO_4 from 16 to 800 mM over 60 min at a flow rate of 0.5 mL/min at room temperature. The eluate was monitored using a UV detector, SPD-20A (Shimadzu Co., Kyoto, Japan), with absorbance at 260 nm. Each nucleotide was identified by comparison of the retention time of the standards. The amount of APS and PAPS in each sample was calculated on the basis of the peak area in the chromatogram.

Results

Clinical Findings

Thirteen patients from 10 families were included in the study (Supp. Table S1). All patients, except one (P13), were from Turkey. The parents of P13 were cousins from Lebanon and Syria. All patients, except one, were consanguineous. There were three pairs of siblings. Five were men and eight were women. All patients were noticed to have the disease between the ages of 2 and 5 years.

All had normal mental and motor developmental milestones and normal facies. All, except one (P3), had postnatal onset of short-trunk short stature (<third percentile), with normal birth length and weight. Arm span was greater than height in all patients, whereas the upper/lower segment ratio was greater than one in three patients. Body weight was not as small relative to height, with only two patients below the third percentile. A short neck and broad chest were found in about half of the patients. All, except one (P12), had varying types of spinal deformities; lumbar and thoracic scoliosis were found in six and five patients, respectively. The proximal interphalangeal joints (PIPJs) were broad in all patients. Pes planus was found in eight of the 12 patients. Genu varum and cubitus valgus were found in several patients (Supp. Table S1). Except for a missing incisor in P11, no patients had dental abnormalities such as oligodontia or enamel hypoplasia. Moreover, none had ophthalmologic abnormalities, including corneal opacities.

Six patients underwent an endocrinologic examination. Two (P1 and P9) showed signs of excess androgen such as hypertrichosis and acne. Their endocrine workups were normal. One (P11) had premature adrenarche, but she did not have an endocrine workup. P13 had a history of precocious puberty, but no signs of androgen excess; her serum DHEA level was high. Three patients had recurrent abdominal pain, and serum anti-gliadin immunoglobulin G level significantly increased in two of them.

Radiographic Findings

Key radiographs were available for all patients (Supp. Table S1). All radiographs were taken after 4 years of age. In 11 of the 13 patients, radiographs from adolescence were available. Radiographs from childhood were available for five patients.

All patients had platyspondyly with rectangular vertebra, irregular end plates, overfaced pedicles, scoliosis, broad ilia, and short femoral necks. Scoliosis was mild (Cobb angle <40°) in most patients. All had narrow disk spaces, except for P8, whose radiographic examinations were only available at 5 years of age and earlier. Lumbar canal stenosis and bulging of intervertebral discs, juxtaphyseal striation of the proximal femur, prominent longitudinal trabecula of the femoral neck, broad proximal phalangeal ends, broad metacarpals, and brachymetacarpy were noted in most patients. Mild metaphyseal abnormalities of the long bones, other than those of the proximal femur, were found in nine of the 13 patients, whereas epiphyseal abnormalities of the long bones were not found, except in P7 who showed flattening of the proximal femoral epiphysis. Mild precocious calcification of costal cartilage was found only in P9. No

Table 1. *PAPSS2* Mutations in the Autosomal Recessive Brachyolmia

Family ID	Position in gene	Mutation	
		Nucleotide change	Amino acid change
F1	Exon 3	c.227T>A	p.L76Q
	Intron 4	c.520+2T>A	p.R129Lfs*25[a]
F2	Exon 10	c.1222+1G>A	p.V364Rfs*18[a]
F3	Exon 3	c.337dup[b]	p.A113Gfs*18
F4	Intron 4	c.520+2T>A	p.R129Lfs*25[a]
F5	Intron 4	c.520+2T>A	p.R129Lfs*25[a]
F6	Exon 12	c.1619T>A	p.V540D
	Exon 5	(c.547G>A)[c]	p.E183K
F7	Exon 5	c.629_630dup	p.Q211Cfs*11
F8	Exon 2	c.128G>A	p.C43Y
F9	Intron 1	c.27+3A>C	(First ATG codon is in exon 1)
F10	Exon 3	c.372del	p.F125Sfs*24

The nucleotide changes are shown with respect to *PAPSS2* mRNA sequence (NM_001015880.1). The corresponding predicted amino acid changes are numbered from the initiating methionine residue.
[a]Not confirmed experimentally.
[b]The same mutation has been reported previously (Miyake et al., 2012).
[c]Most likely to be a polymorphism from in vitro functional assay (and presence of c.1619T>A).

patient had early osteoarthritic changes. When a patient's bone age was estimated to within ±2 standard deviations (SDs) of the bone age according to the patient's chronological age [Greulic and Pyle, 1959], it was considered normal. The bone age was within the normal limit in six patients, advanced in five patients, and delayed in one patient.

Identification of *PAPSS2* Variants

By direct sequencing, we screened all 13 coding exons of *PAPSS2* and their exon–intron boundaries in 10 probands. *PAPSS2* variants likely to be disease-causing mutations were found in both alleles of all patients (Table 1). One was a compound heterozygote, and the others were homozygous for the variants. c.520+2T>A variants were found in three apparently unrelated families. Altogether, 10 possible mutations were found, and nine of those were novel. There were three splice donor-site variants, four missense variants, and three insertion/deletion variants in coding regions. The splice site and insertion/deletion variants were all predicted to cause premature stop codons, most likely leading to nonsense mutation-mediated RNA decay. The missense variants were predicted to have a damaging function against the gene product. Cosegregation of mutations in the families was confirmed by sequencing and/or invader assay when DNAs of the family members were available. No variants were present in ethnically matched controls or in public databases. c.547G>A (E183K) and c.1619T>A (V540D) were both identified in F6, and cosegregated with the disease phenotype in the family. Both were not in the public database for polymorphism. Therefore, it was difficult to determine which of the two variants caused the disease phenotype.

Functional Characterization of *PAPSS2* Missense Variants

We evaluated the causality of the *PAPSS2* missense variants by measuring their PAPS synthase activities. The expression vectors for the wild type and the missense variants, c.128G>A (C43Y), c.227T>A (L76Q), c.547G>A (E183K), and c.1619T>A (V540D), were constructed, and the recombinant PAPSS2 proteins were expressed in COS-7 cells (Fig. 2A). Although a peak from PAPS was detected in the wild type PAPS (Fig. 2B), no enzyme activity was found in C43Y, L76Q, or V540D variants (Fig. 2C and E) or in the empty vector (data not shown), indicating that these mutants abolish the biosynthetic ability of the active sulfate, PAPS. The E183K variant showed similar activity to the wild type (Fig. 2D and E). Thus, E183K is likely an innocent polymorphism, whereas C43Y, L76Q, and V540D are disease-causing loss-of-function mutations.

Discussion

In this study, we screened *PAPSS2* mutations in 10 unrelated families and found mutations in all. Together with previous studies [Faiyaz ul Haque et al., 1998; Miyake et al., 2012; Noordam et al., 2009], 18 types of *PAPSS2* mutations have been identified in 16 unrelated families. A missense mutation, c.985C>T (T48R), has been found in spondylodysplasia and premature pubarche [Noordam et al., 2009]. An in vitro functional assay showed that the mutant PAPSS2 has only 6% of the activity of the wild type PAPSS2. Similarly, in our study, all mutations were considered loss-of-function mutations based on in silico analyses and in vitro experiments. Thus, all *PAPSS2* mutations are considered to cause loss of PAPSS2 function.

Including the findings of six patients with previously identified *PAPSS2* mutations [Miyake et al., 2012], the phenotypic characteristics of *PAPSS2*-brachyolmia are short trunk, short stature, normal intelligence and facies, spinal deformity, and broad PIPJ. Short stature becomes conspicuous after infancy; it is less severe than in most patients with other skeletal dysplasias, but medical advice is usually sought during late childhood or adolescence. A relative increase in arm span is typical. The upper/lower segment ratio is below one in patients with no associated limb deformities, including genu varum. Spinal deformity includes thoracic or lumbar scoliosis in most patients, but kyphosis and lumbar lordosis could occur. Most of the spinal deformities are not so severe as to warrant surgical treatment. Pes planus, cubitus valgus, and genu varum are common limb deformities.

Radiographic features include platyspondyly with rectangular vertebral bodies and irregular end plates, overfaced pedicles, broad ilia, metaphyseal changes of the proximal femur, and dysplasia of short tubular bones. None of the characteristics of SEMD Pakistani type, including enlarged joints with deformity, delayed epiphyseal ossification at the hip and knee, and precocious osteoarthritic changes of the large and small joints [Ahmad et al., 1998; Faiyaz ul Haque et al., 1998], were noted in other families.

Spinal disorders, including the rectangular vertebral body, fit the conventional clinical classification of type 1 brachyolmia [Rock et al., 2008], which are clearly differentiated from other clinical types of brachyolmia. The Hobaek and Toledo forms of type 1 brachyolmia are discriminated by the presence of corneal opacity and premature calcification of costal cartilage in the latter [Mourao et al., 1973; Shohat et al., 1989; Toledo et al., 1978]. In the present series, corneal opacity was not found. Premature calcification of costal cartilage was found only in a 15-year-old girl (P9) in this study, whereas it was found in three patients in our previous series [Miyake et al., 2012]. It should be noted that Family 3 in this series and Family 1 in our previously reported series [Miyake et al., 2012] had the same homozygous mutation (c.337dup) (Table 1). There were only a few phenotypic differences between the five patients of the two families harboring the identical *PAPSS2* genotype. Precocious calcification of costal cartilage was found in two patients in Family 1 and none in Family 3. The differences regarding the calcification of costal cartilage is likely to be attributable to the ages of

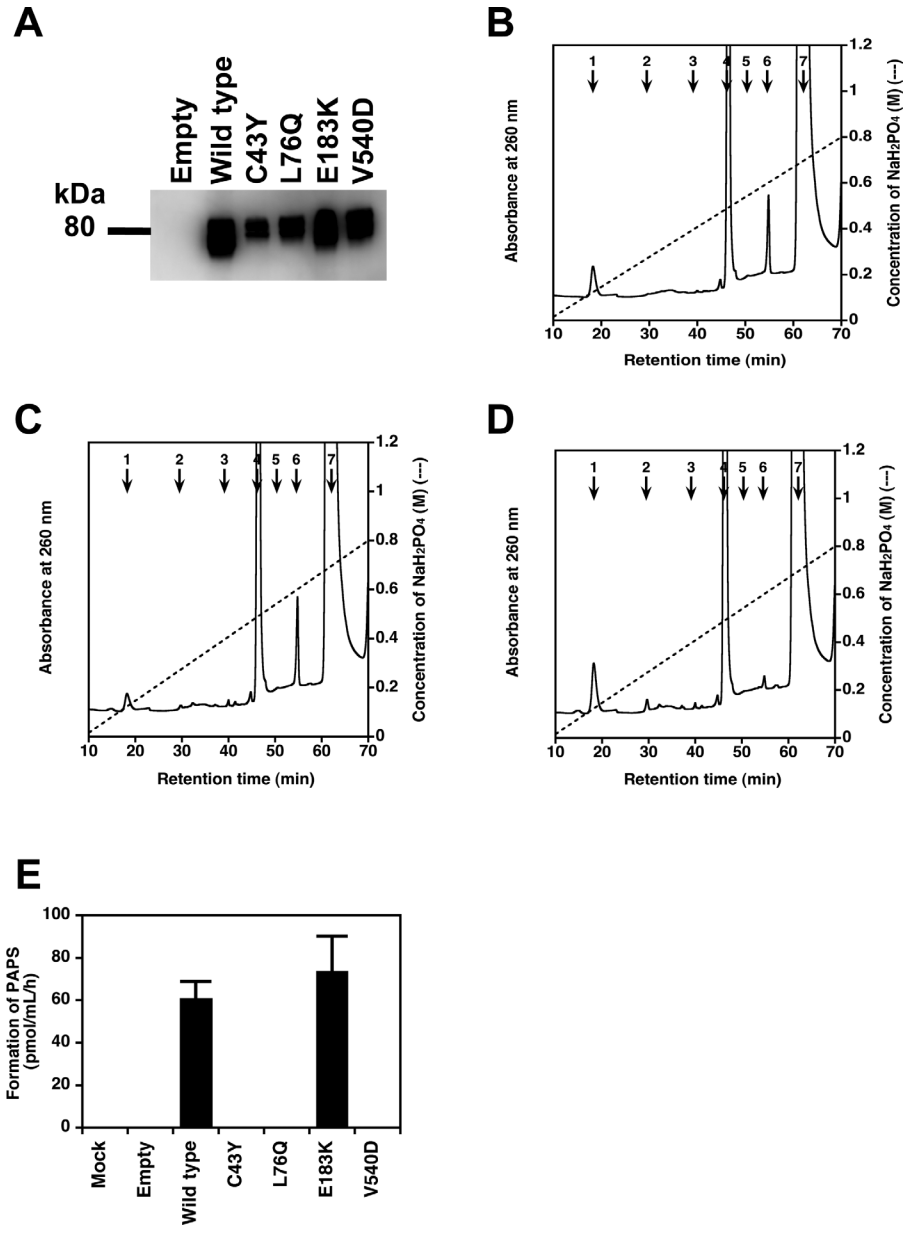

Figure 2. Decreased PAPSS2 enzyme activities of the missense mutations in the patients in vitro. **A:** Western blotting of the recombinant FLAG–PAPSS2 (wild type and mutants). The recombinant PAPSS2 was transiently expressed in COS-7 cells, separated by 7.5% SDS-polyacrylamide gel electrophoresis, and detected with horseradish peroxidase-conjugated anti-FLAG antibody. "Empty" indicates the conditioned medium from COS-7 cells transfected with an empty vector. **B–F:** PAPS synthase activity of the soluble form of recombinant PAPSS2 proteins (wild type and mutants). Anion-exchange HPLC of the reaction products prepared using the soluble form of recombinant PAPSS2 of wild type (B), C43Y (C), L76Q (D), E183K (E), and V540D (F), and ATP, and inorganic sulfate as substrates. Representative chromatograms from individual reaction products are shown in the figure. The reaction products were separated by anion-exchange HPLC on an amine-bound silica PA-G column using a linear gradient of NaH_2PO_4 as indicated by the dashed line. The elution positions of authentic ribonucleotides are indicated by numbered arrows: 1, 5′-AMP; 2, 3′-AMP; 3, APS; 4, ADP; 5, PAP; 6, PAPS; 7, ATP. **G:** Comparison of the PAPS synthase activity of the soluble form of the recombinant PAPSS2 (mean ± SD, $n = 3$). The reaction products were analyzed by anion-exchange HPLC (B–F). Mock and empty indicate the PAPS synthase activity of the conditioned media of COS-7 cells transfected without and with an empty vector, respectively. *, $P < 0.001$ by Student's *t*-test.

the patients at radiographic examination; in the three patients, calcification of costal cartilage was found in adult patients [Miyake et al., 2012], whereas radiographic evaluation after 20 years of age was available for only one patient in the present series. Abnormal chondroitin sulfation metabolism in the Toledo forms of brachyolmia has been reported, including undersulfation of chondroitin-6-sulfate in the urine [Toledo et al., 1978] and low PAPS-chondroitin sulfate sulfotransferase activity in the serum [Mourao et al., 1981]. These findings indicate that *PAPSS2*-brachyolmia corresponds to conventional clinical classification of type 1 brachyolmia; the Hobaek and Toledo forms are variations of the *PAPSS2* mutation phenotype.

Broad ilia and short femoral necks are characteristic findings of *PAPSS2*-brachyolmia. The latter usually associates juxtaphyseal striation and/or prominent longitudinal trabeculae, which have been described in the Hobaek type brachyolmia [Hoo and Oliphant, 2003;

Ikegawa et al., 1995]. This feature most likely results because of the disorder of the growth plate of the proximal femur.

Brachyolmia does not exist on its own; some degrees of metaphyseal and/or epiphyseal involvements of the long tubular bones usually accompany this condition [Kozlowski et al., 1982]. In this series, all patients had abnormalities in the metaphysis of the proximal femur, and more than two-thirds had metaphyseal dysplasia of the long bones (other than the proximal femur), although there was no overt epiphyseal dysplasia in the long tubular bones, except for in P7. While disorders of the axial skeleton (spine, pelvis, and hip) are very similar, disorders of the long and short tubular bones (other than the proximal femur) are very variable among patients. They were variable even in the same family and among patients with the same mutation. It is of note that one patient (P11) showed metaphyseal dysplasia of the long bones at 5 years of age, but it diminished with age. The disorders of the short tubular bones are constant, but also very variable among patients, except for broad PIPJs.

We have previously reported on advanced bone age as a feature of *PAPSS2*-brachyolmia; however, it is denied by the present study. More than half of the patients did not show advanced bone age, and one patient even showed delayed bone age. Notably, advanced bone age was negative even in a patient with positive signs of androgen excess (P1). Her bone age was estimated at 13 years when her chronologic age was 14 years and 2 months.

Three patients (one man and two women) in this study exhibited signs of androgen excess; another patient showed increased serum DHEA, although she did not show signs of androgen excess. We have also recognized increased serum DHEA without overt clinical signs of androgen excess in a patient [Miyake et al., 2012]. Disruption of PAPSS2 activity results in apparent DHEA sulfotransferase (SULT2A1) deficiency. Disruption of SULT2A1 activity is hypothesized to result in decreased inactivation of DHEA to DHEA sulfate, thereby fueling the activation of androgens, resulting in androgen excess [Idkowiak et al., 2011]. Therefore, the association of *PAPSS2* mutation with abnormal androgen metabolism previously reported in a patient with spondylodysplasia and premature pubarche [Noordam et al., 2009] is not fortuitous. It remains an enigma why only a minority of patients present with signs of androgen excess. Further endocrinologic studies are necessary to better understand *PAPSS2*-brachyolmia.

Acknowledgments

We thank the patients and their family for their help to the study. We also thank the Japanese Skeletal Dysplasia Consortium and Ms. Tomoko Kusadokoro for technical assistance.

Conflict of interest: The authors declare no competing financial interests.

References

Ahmad M, Haque MF, Ahmad W, Abbas H, Krakow D, Rimoin DL, Lachman RS, Cohn DH. 1998. Distinct, autosomal recessive form of spondyloepimetaphyseal dysplasia segregating in an inbred Pakistani kindred. Am J Med Genet 78:468–473.

Dai J, Cho TJ, Unger S, Lausch E, Nishimura G, Kim OH, Superti-Furga A, Ikegawa S. 2010. TRPV4-pathy, a novel channelopathy affecting diverse systems. J Hum Genet 55:400–402.

Faiyaz ul Haque M, King LM, Krakow D, Cantor RM, Rusiniak ME, Swank RT, Superti-Furga A, Haque S, Abbas H, Ahmad W, Ahmad M, Cohn DH. 1998. Mutations in orthologous genes in human spondyloepimetaphyseal dysplasia and the brachymorphic mouse. Nat Genet 20:157–162.

Fuda H, Shimizu C, Lee YC, Akita H, Strott CA. 2002. Characterization and expression of human bifunctional 3′-phosphoadenosine 5′-phosphosulphate synthase isoforms. Biochem J 365:497–504.

Greulich WW, Pyle SI. 1959. What constitutes a significant deviation from normal? In: Greulich WW, Pyle SI, editors. *Radiographic atlas of skeletal development of the hand and wrist. 2e. Palo Alto, CA*: Stanford University Press. p 48–57.

Heckman KL, Pease LR. 2007. Gene splicing and mutagenesis by PCR-driven overlap extension. Nat Protoc 2:924–932.

Hoo JJ, Oliphant M. 2003. Two sibs with brachyolmia type Hobaek: five year-follow-up throught puberty. Am J Med Genet A 116A:80–84.

Idkowiak J, Lavery GG, Dhir V, Barrett TG, Stewart PM, Krone N, Arlt W. 2011. Premature adrenarche: novel lessons from early onset androgen excess. Eur J Endocrinol 165:189–207.

Ikegawa S, Nakamura K, Nakamura S, Nagano A. 1995. Brachyolmia: a report of two cases. Pediatr Orthop 15:105–107.

Kozlowski K, Beerner FA, Bens G, Dijkstra PF, Iannaccone G, Emons D, Lopez-Ruiz P, Masel J, van Nieuwenhuizen O, Rodriguez-Barrionuevo C. 1982. Spondylometaphyseal dysplasia (report of 7 cases and essay of classification). Prog Clin Biol Res 104:89–101.

Lindsay J, Wang LL, Li Y, Zhou SF. 2008. Structure, function and polymorphism of human cytosolic sulfotransferases. Curr Drug Metab 9:99–105.

Miyake N, Elcioglu NH, Iida A, Isguven P, Dai J, Murakami N, Takamura K, Cho TJ, Kim OH, Hasegawa T, Nagai T, Ohashi H, et al. 2012. PAPSS2 mutations cause autosomal recessive brachyolmia. J Med Genet 49:533–538.

Mizumoto S, Ikegawa S, Sugahara K. 2013. Human genetic disorders caused by mutations in the genes encoding biosynthetic enzymes for sulfated glycosaminoglycans. J Biol Chem 288:10953–10961.

Mourao PAS, Kato S, Donnelly PV. 1981. Spondyloepiphyseal dysplasia, chondroitin sulfate type: a possible defect of PAPS-chondroitin sulfate sulfotransferase in humans. Biochem Biophys Res Commun 98:388–396.

Mourao PAS, Toledo SPA, Nader HB, Dietrich CP. 1973. Excretion of chondroitin sulfate C with low sulfate content by patients with generalized platyspondyly (brachyolmia). Biochem Med 7:415–423.

Noordam C, Dhir V, McNelis JC, Schlereth F, Hanley NA, Krone N, Smeitink JA, Smeets R, Sweep FC, Claahsen-van der Grinten HL, Arlt W. 2009. Inactivating PAPSS2 mutations in a patient with premature pubarche. N Engl J Med 360:2310–2318.

Ohnishi Y, Tanaka T, Ozaki K, Yamada R, Suzuki H, Nakamura Y. 2001. A high-throughput SNP typing system for genome-wide association studies. J Hum Genet 46:471–477.

Rock MJ, Prenen J, Funari VA, Funari TL, Merriman B, Nelson SF, Lachman RS, Wilcox WR, Reyno S, Quadrelli R, Vaglio A, Owsianik G, et al. 2008. Gain-of-function mutations in TRPV4 cause autosomal dominant brachyolmia. Nat Genet 40:999–1003.

Shohat M, Lachman R, Gruber HE, Rimoi DL. 1989. Brachyolmia: radiographic and genetic evidence of heterogeneity. Am J Med Genet 33:209–219.

Stelzer C, Brimmer A, Hermanns P, Zabel B, Dietz UH. 2007. Expression prolie of Papss2 (3′-phosphoadenosine 5′-phosphosulfate synthase 2) during cartilage formation and skeletal development in the mouse embryo. Dev Dyn 236:1313–1318.

Sugahara K, Schwartz NB. 1979. Defect in 3′-phosphoadenosine 5′-phosphosulfate formation in brachymorphic mice. Proc Natl Acad Sci USA 76:6615–6618.

Sugahara K, Schwartz NB. 1982a. Defect in 3′-phosphoadenosine 5′-phosphosulfate synthesis in brachymorphic mice. I. Characterization of the defect. Arch Biochem Biophys 214:589–601.

Sugahara K, Schwartz NB. 1982b. Defect in 3′-phosphoadenosine 5′-phosphosulfate synthesis in brachymorphic mice. II. Tissue distribution of the defect. Arch Biochem Biophys 214:602–609.

Toledo SPA, Mourao PAS, Lamego C, Alves CAR., Dietrich CP, Assis LM, Mattar E. 1978. Recessively inherited, late onset, spondylar dysplasia and peripheral corneal opacity with anomalies in urinary mucopolysaccharides: a possible error of chondroitin-6-sulfate synthesis. Am J Med Genet 2:385–395.

Venkatachalam KV. 2003. Human 3′-phosphoadenosine 5′-phosphosulfate (PAPS) synthase: biochemistry, molecular biology and genetic deficiency. IUBMB Life 55:1–11.

Warman ML, Cormier-Daire V, Hall C, Krakow D, Lachman R, LeMerrer M, Mortier G, Mundlos S, Nishimura G, Rimoin DL, Robertson S, Savarirayan R, et al. 2011. Nosology and classification of genetic skeletal disorders: 2010 revision. Am J Med Genet A 155A:943–968.